Eos, Transactions, American Geophysical Union, Vol. 72, No. 15, April 9, 1991, Pages 169, 174–175

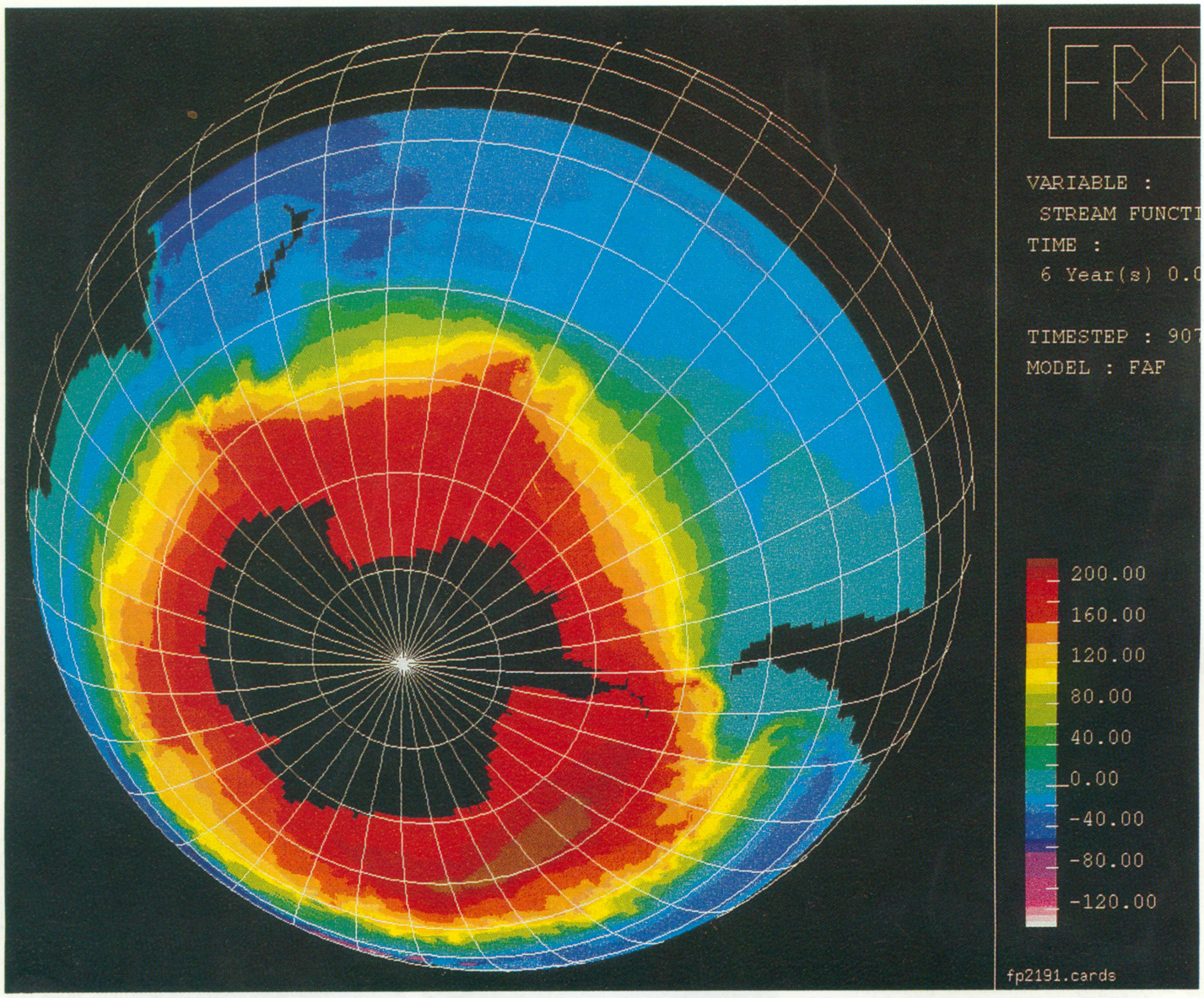

Fig. 1. Contours of stream function (depth integrated transport) in units of $10^6 m^3 s^{-1}$ at the end of 6 years.

An Eddy-Resolving Model of the Southern Ocean

The FRAM Group

Existing numerical models used for climate prediction have horizontal resolutions (that is, grid spacings) of several hundred kilometers. Regional numerical models of areas such as the Southern Ocean use a model grid with a horizontal resolution of 100 km or more. Both of these resolutions are far too coarse to correctly represent either the major ocean currents (the Gulf Stream is typically 50 km wide) or the oceanic eddy field (eddies of 100–200 km diameter). The models do not properly reproduce detailed field observations, and they are probably adequate for climate prediction only if suitable parameterizations of the eddy field are included. Although the computer costs are high, models that can resolve these features should be substantially more realistic, predict climate change better, and provide better insight into the physics controlling the ocean.

We have chosen to study the Southern Ocean and the Antarctic Circumpolar Current because of the area's importance for climate (the Southern Ocean provides the only con-

0096/3941/7215/91/169/$01.00

The FRAM Group: David J. Webb, David Beckles, Beverly A. de Cuevas, Raymond Pollard—Institute of Oceanographic Sciences, Deacon Laboratory, Godalming, Surrey, GU8 5UB; Peter D. Killworth, Max Rowe, Richard Offiler—Robert Hooke Institute, Clarendon Laboratory, University of Oxford, and Institute of Oceanographic Sciences, Deacon Laboratory; Stephen Maskell, Andrew Willmott—Department of Mathematics, Exeter University; Kelvin Richards, Neil Wells—Department of Oceanography, Southampton University; John Marshall—Department of Atmospheric Physics, Imperial College, London; Peter Wadhams, Robin Williams—Scott Polar Research Institute, University of Cambridge; John Johnson, Grant Bigg, David Stevens—Department of Mathematics, University of East Anglia, Norwich.

nection between the main ocean basins) and because models without eddies cannot account for the momentum or vorticity budget of the Antarctic Circumpolar Current. However, computer power does not yet permit the long integrations necessary to adequately represent the thermohaline circulation.

Accordingly, we have carried out a numerical integration of an eddy-resolving model of the Southern Ocean as part of a UK project to improve the ocean models used for climate prediction. For the first 6 years of integration the model was spun up using a long time-scale, robust diagnostic method. The resulting temperature, salinity, and velocity fields are in good qualitative agreement with available observations. The model results (Figure 1) show that the Circumpolar Current contains embedded high velocity filaments that follow the bottom topography of the ocean. One filament, passing through the Udintsev Fracture Zone in the South Pacific, transports $100 \times 10^6 m^3 s^{-1}$ through a channel less than 130 km wide. The model reproduces the eddies formed by the Agulhas Current and shows that these transport 0.2 PW of heat from the Indian Ocean into the Atlantic Ocean.

Model Description

The eddy-resolving model used for the present study is based on that of *Semtner* [1974] and *Cox* [1984], with 32 vertical levels and a horizontal grid spacing of 1/2° in the east-west direction and 1/4° north-south. This gives a grid spacing at 60°S of about 27 km. The model uses viscosity coefficients of $2 \times 10^2 m^2 s^{-1}$ horizontally and $10^{-4} m^2 s^{-1}$ vertically. The diffusion coefficients for temperature and salinity are $10^2 m^2 s^{-1}$ horizontally and $0.5 \times 10^{-4} m^2 s^{-1}$ vertically. The topography is based on the DBDB5 depth data set [*U.S. Naval Oceanographic Office*, 1983], smoothed to a one-degree grid to prevent topographic instabilities [*Killworth*, 1987]. Linear bottom friction is used, corresponding to an e-folding time of 50 days for a 4000-m ocean. The boundary condition used at the northern open boundary is that proposed by *Stevens* [1990].

The model was first initialized using the *Levitus* [1982] temperature and salinity fields (a smoothed data set based on field measurements), and zero velocity. This method was found to be unstable due to barotropic (that is, depth-independent) topographic modes trapped near Kerguelen and New Zealand, which are driven by the bottom pressure torque. (This difficulty did not occur in the U.S. Community Modeling Effort's North Atlantic calculation, probably due to the weaker topographic and density gradients employed [*Bryan and Holland*, 1989]). The system was reinitialized as a cold (−2°C), saline (36.69‰), motionless fluid, and the temperature and salinity fields then dynamically relaxed to the Levitus data. During the first 2 years and 160 days, the relaxation time scales are 180 days for the top 140 m and 540 days for the deeper levels. From that time up to 6 years, the time scale is 360 days throughout. This is equivalent to the normal robust diagnostic scheme [*Sarmiento and Bryan*, 1982], except that the relaxation is so weak that it permits eddies, fronts, and other realistic features to develop. *Semtner and Chervin* [1988] retain this relaxation below the thermocline during their entire run. For times beyond 6 years (not reported here), our model ocean runs free from relaxation terms. However, the results given here will demonstrate the value of what can be thought of as an assimilation of the Levitus data into a dynamical model.

The model is forced by annual mean winds (*Hellerman and Rosenstein*, 1983). These are built up linearly during the third year of the run from zero to their steady value.

Model Behavior

During the first few days of the integration, large-scale barotropic Rossby waves are observed, but by day 10 (Figure 2) the main feature of the flow is a rudimentary Circumpolar Current, whose amplitude, measured by transport through Drake Passage, grows roughly linearly with time. The density variation, being relaxed to the Levitus data, also grows linearly with time for the first 200 days (until advective effects become sufficiently large to modify the density response). Figure 2 shows clearly that the combination of the density field and the topography therefore determines most of the barotropic circulation, even down to details such as the pinching behavior of the Circumpolar Current near fracture zones (see Figure 1).

The rapid response in time probably occurs because all barotropic basin modes are high frequency (that is, with frequency of order of the Coriolis parameter). After 3 years, the transport through Drake Passage is $150 \times 10^6 m^3 s^{-1}$. When the winds are added, the model again responds in less than 10 days, by increasing the rate of change of the transport—again showing the short time scales of the barotropic modes. At the end of the third year, when the wind-forcing steadies, the transport is $180 \times 10^6 m^3 s^{-1}$, about $23 \times 10^6 m^3 s^{-1}$ larger than predicted by extrapolating the transport calculated before the winds were added. Between years five and six the transport, the total kinetic energy of the model, and other diagnostics settle down, indicating that the momentum budget of the model is near its asymptotic state.

At the end of 6 years (Figure 2), the total Drake Passage transport is $195 \times 10^6 m^3 s^{-1}$. This is larger than the observed value of $130 \times 10^6 m^3 s^{-1}$ [*Whitworth et al.*, 1982]. The baroclinic (that is, depth-dependent) component of the transport, which is determined primarily by the north-south density gradient, is very similar to that observed. The difference in barotropic transport can be accounted for by an excess eastward bottom velocity of $0.021\ ms^{-1}$. This overestimate seems endemic in fine resolution models (see *Semtner and Chervin*'s almost identical 1988 estimate). Coarse ocean models vary in their ability to reproduce the correct transport; *Mikolajewicz and Maier-Reimer*'s [1990] model has little difficulty in reproducing observed transports, whereas *Cox*'s [1975] world ocean calculation yields values similar to ours. This shows the difficulty that general circulation models have in computing bottom pressure drags and torques in the presence of topography; yet these terms seem to be vital for the dynamics of the Antarctic Circumpolar Current [*Johnson and Bryden*, 1989].

The velocity field in this passage has a banded structure (Figure 3) similar to that observed experimentally [*Whitworth et al.*, 1982]. (We show instantaneous values to permit comparison with observations.) Here, as elsewhere, the model sharpens the Levitus temperature field, to produce a series of fronts. In the passage, three of these fronts correspond to eastward jets. A well-defined Polar Front is found at 63°S, and a strong Subantarctic Front at 57.5°S. In between, a weaker front is observed, together with a recirculation feature, containing the only region of westward currents. (The two main fronts are also reproduced in the global model of *Semtner and Chervin* [1988], which has a resolution of 0.5° in the north-south direction and 20 levels in the vertical.) Note that although the current structure near the fronts is predominantly baroclinic, there is a significant barotropic component. Away from the Drake Passage, the bottom velocity is eastward almost everywhere, in contradiction to a recent inverse calculation [*Olbers and Wenzel*, 1990].

Analysis of the stream function (Figure 2) shows that topographic features dominate the path of the Circumpolar Current. In the South Pacific the model shows that the current crosses the isolated Pacific-Antarctic

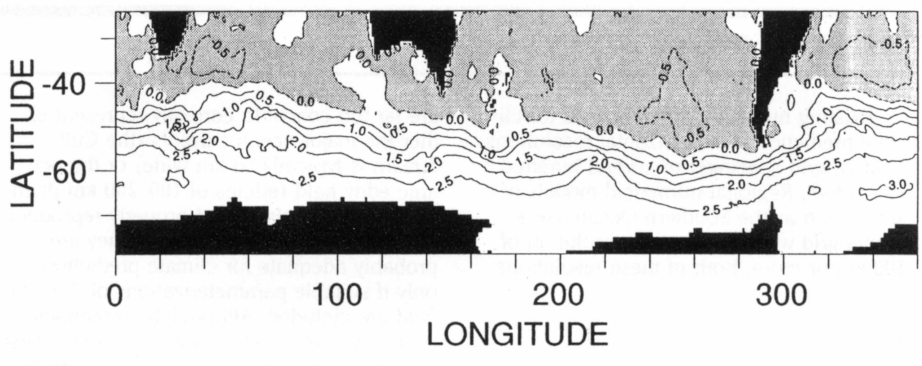

Fig. 2. Contours of stream function (depth integrated transport) in units of $10^6 m^3 s^{-1}$ at the end of 10 days. Contour interval 0.5; shaded values negative.

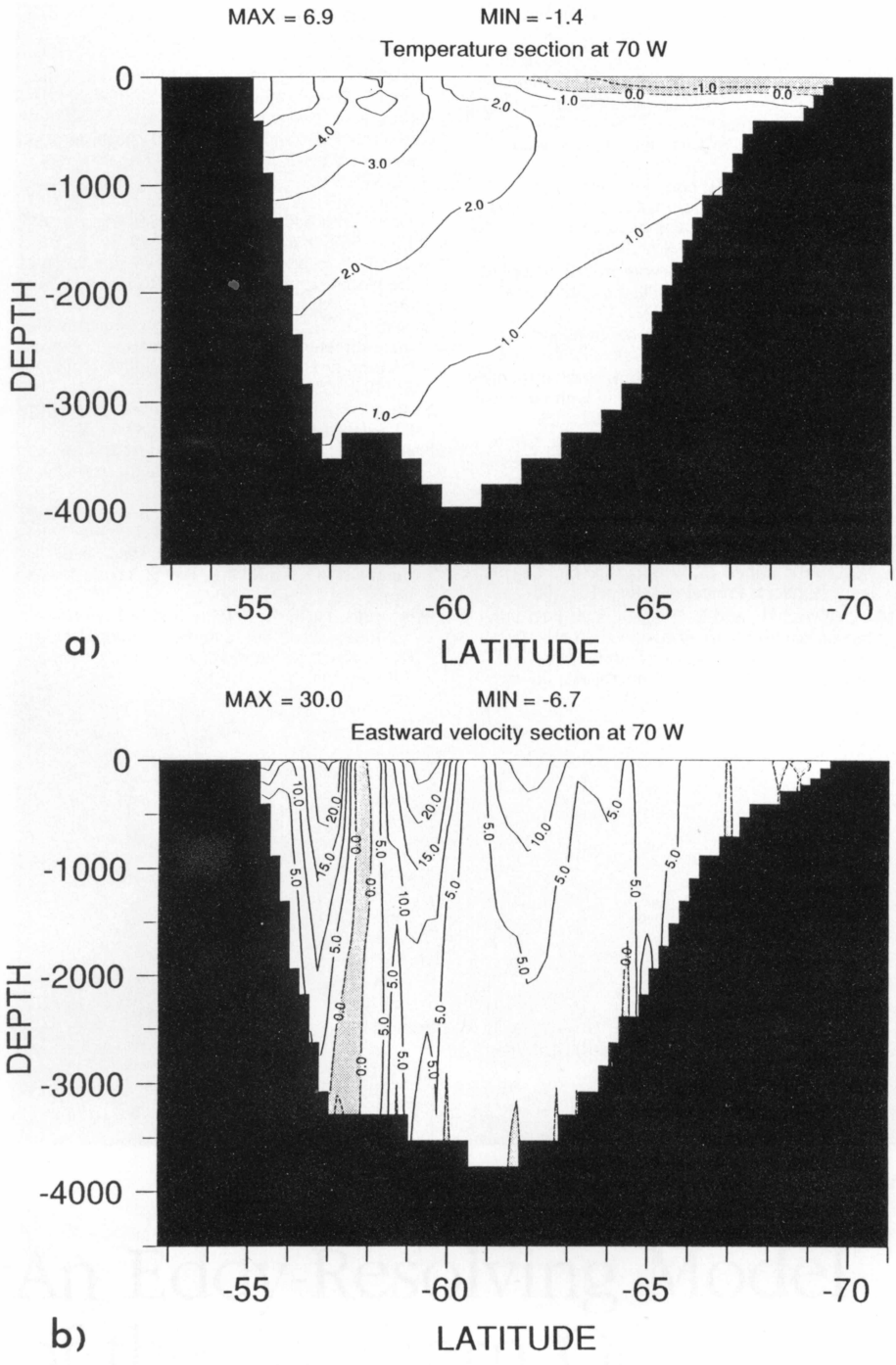

Fig. 3. Contours of (a) temperature and (b) eastward velocity on a north-south section across the Drake Passage at 70°W at the end of 6 years. Contour intervals: (a) 1°C, (b) 0.05 ms^{-1}. Negative values shaded.

ridge through the Menard, Eltanin, and Udintsev fracture zones. The maximum flow is found at the southernmost Udintsev fracture zone where the current has a total transport of 100 × 10^6m^{3}s^{-1}, through a channel less than 130 km wide. On each side of the region, steering by the topography is evident. In addition, strong eddy activity is observed near the ridge axis, with less visible activity on the neighboring abyssal plains. This is in qualitative agreement with the GEOSAT observations of surface variability [*Chelton et al.*, 1990].

Currents

The distribution of current speeds shows narrow bands of strong currents (above 0.3 ms^{-1}). These too are generally associated with strong topographic features in the path of the Circumpolar Current. To the east of Drake Passage, one such feature is the Falkland Current, which plays the role of a western boundary current as the axis of the Circumpolar Current shifts from 60°S to 45°S. Other current bands may be distinguished near Kerguelen and south of the Campbell Plateau off New Zealand. The transport of the Falkland Current is 67 × 10^6m^{3}s^{-1} at 48°S and 42 × 10^6m^{3}s^{-1} at 44°S. (*Stamma*'s [1989] observations of just the baroclinic part of the flow give 10 × 10^6m^{3}s^{-1} at 46°S.)

The Brazil Current has a barotropic flux of 26 × 10^6m^{3}s^{-1} at 33°S (17.5 × 10^6m^{3}s^{-1} is observed by *Gordon and Greengrove* [1986]), increasing to 30 × 10^6m^{3}s^{-1} in the recirculation region at 35°S. The model shows the current separating from the coast at this latitude, in good agreement with observations. The East Australian Current has a flux of 37 × 10^6m^{3}s^{-1} at 30°S. This is slightly higher than observed, possibly the result of the model's neglect of the Pacific-Indian Ocean through-flow north of Australia. The current separates from the coast at 32°S, and generates a series of eddies that drift southward, in good agreement with observations [*Boland and Hamon*, 1970].

The most eddy-energetic region is the Agulhas Current off South Africa. In the north, its transport is 57 × 10^6m^{3}s^{-1} at 30°S. This compares favorably with observations [*Toole and Raymer*, 1985; *Grundlingh*, 1980] of 44 × 10^6m^{3}s^{-1} to 60 × 10^6m^{3}s^{-1}. The flux increases to 89 × 10^6m^{3}s^{-1} at 35°S at the start of the recirculation region. During the spinup of the model, eddies were not formed until the transport in the Agulhas Current exceeded 50 × 10^6m^{3}s^{-1}. During the later part of the spinup, a new eddy formed roughly every 160 days and drifted into the South Atlantic with a speed of 0.04 ms^{-1}. At the moment of separation, the total transport around an eddy is 130 × 10^6m^{3}s^{-1}.

The total heat content of an eddy relative to its surroundings is 2.6 × 10^{21} Joules, and its volume is about 1.4 × 10^{14}m^3. This yields a total heat flux from the Indian Ocean to the Atlantic, due to the eddies, of around 0.2 PW and a mass flux of 10 × 10^6m^{3}s^{-1}.

These Agulhas eddies decay rapidly once in the South Atlantic, the e-folding time for decay of the transport within each eddy being less than 1 year. This is more rapid than the expected lateral diffusion time of 3 years, and is almost certainly due to the rapid potential energy loss by relaxation to Levitus used in this part of the model run. Further south, we find that the eddies generated by the Circumpolar Current propagate only short distances, again probably due to the imposed relaxation. (The decay was much reduced when the run was continued with the relaxation removed.)South of the Circumpolar Current, the main feature is the Weddell Gyre, with a total transport of 26 × 10^6m^{3}s^{-1}. The model shows that it extends eastwards as far as the Kerguelen Plateau. The Ross Sea also forms a cyclonic gyre, with a transport of 7 × 10^6m^{3}s^{-1}, extending from 160°E to 140°W.

Conclusions

The present model has shown that by going to an eddy-resolving scale, the performance of ocean models can be significantly improved. Some of the important processes involved in climate change, such as deep convection at high latitudes, may still not be

adequately resolved, but the results are a significant improvement over those of non-eddy resolving models.

Acknowledgments

The FRAM Community Research Project is supported by the Natural Environment Research Council. Computations were performed at the Atlas Computer Laboratory. Valuable graphical work was provided by Andrew Anson, Jeffrey Blundell, and Tim Hateley.

References

Boland, F. M., and B. V. Hamon, The East Australian Current, 1965–1968, *Deep Sea Res., 17*, 777, 1970.

Bryan, F. O., and W. R. Holland, A high resolution simulation of the wind- and thermohaline-driven circulation in the North Atlantic Ocean, in *Parameterisation of Small-Scale Processes, Proc. of 'Aha Huliko'a Winter Workshop 1989*, edited by P. Muller and D. Henderson, 99–116, Hawaii Institute of Geophysics, Hawaii, 1989.

Chelton, D. B., M. G. Schlax, D. L. Wilfer, and J. G. Richman, Geosat altimeter observations of the surface circulation of the Southern ocean, *J. Geophys. Res., 95*, 17877, 1990.

Cox, M. D., A baroclinic numerical model of the world ocean: preliminary results, in *Numerical Models of Ocean Circulation*, edited by R. O. Reid, A. R. Robinson, and K. Bryan, 107–120, National Academy of Sciences, Washington, D.C., 1975.

Cox, M. D., A primitive equation, three-dimensional model of the ocean, *GFDL Ocean Group Tech. Rep., 1*, Geophysical Fluid Dynamics Laboratory, Princeton Univ., N.J., 1984.

Gordon, A. L., and C. L. Greengrove, Geostrophic circulation of the Brazil-Falkland confluence, *Deep Sea Res., 33*, 573, 1986.

Grundlingh, M. L., On the volume transport of the Agulhas Current, *Deep Sea Res., 27*, 557, 1980.

Hellerman, S., and M. Rosenstein, Normal monthly wind stress over the world ocean with error estimates, *J. Phys. Oceanogr., 13*, 1093, 1983.

Johnson, G. C., and H. L. Bryden, On the size of the Antarctic Circumpolar Current, *Deep Sea Res., 36*, 39, 1989.

Killworth, P. D., Topographic instabilities in level model OGCMs, *Ocean Modelling, 75*, 9, 1987.

Levitus, S., Climatological atlas of the world ocean, *NOAA Prof. Paper, 13*, Geophysical Fluid Dynamics Laboratory, Princeton Univ., N.J., 1982.

Mikolajewicz, U., and E. Maier-Reimer, Internal secular variability in an ocean general circulation model, *Clim. Dynam., 4*, 145, 1990.

Olbers, D., and M. Wenzel, Determining diffusivities from hydrographic data by inverse methods with applications to the Circumpolar Current, in *Ocean Circulation Models: Combining Data and Dynamics*, edited by D. Anderson and J. Willebrand, 95–139, Kluwer Academic Publishers, Dordrecht, Germany, 1990.

Sarmiento, J. L., and K. Bryan, An ocean transport model for the North Atlantic, *J. Geophys. Res., 87*, 394, 1982.

Semtner, A. J., An oceanic general circulation model with bottom topography, *UCLA Dept. of Meteor. Tech. Report, 9*, 99 pp., 1974.

Semtner, A. J., and R. M. Chervin, A simulation of the global ocean circulation with resolved eddies, *J. Geophys. Res., 93*, 15502, 1988.

Stevens, D. P., On open boundary conditions for three dimensional primitive equation ocean circulation models, *Geophys. Astrophys. Fluid Dyn., 51*, 103, 1990.

Stramma, L., The Brazil Current transport south of 23°S, *Deep Sea Res., 36*, 639, 1989.

Toole, J. M., and M. E. Raymer, Heat and fresh water budgets of the Indian Ocean—revisited, *Deep Sea Res., 32*, 917, 1985.

U.S. Naval Oceanographic Office, and the U. S. Naval Ocean Research and Development Activity, DBDB5 (Digital Bathymetric Data Base—5 minute grid), U.S.N.O.O., Bay St. Louis, Mississippi.

Whitworth, T., W. D. Nowlin, and S. J. Worley, The net transport of the Antarctic Circumpolar Current through Drake Passage, *J. Phys. Oceanogr., 12*, 960, 1982.